



Bi Doping Starch-DMAEMA Hydrogel for Efficient Removal of Sr(II)

Esraa A. Alshafei,^a M. Abdel Geleel,^a Ghada A. Mahmoud,^b Nagwa A. Badway,^c Samia.A. Abo Farha^c

^aNuclear fuel cycle dept, Nuclear and Radiological Safety Research center, Egyptian Atomic Energy Authority (EAEA), 3 Ahmed El Zomor St, Nasr city, P.O.B.11762, Cairo, Egypt.

^bPolymer Chemistry Department, (NCRRT), Egyptian Atomic Energy Authority (EAEA), 3 Ahmed El Zomor St, Nasr city, P.O.B.11762, Cairo, Egypt.

^cChemistry Department, Faculty of Science(Girls), Al-Azhar University, Youssef Abas St, Nasr City, P.O.B.11754, Cairo, Egypt.



Abstract

One of the most significant environmental issues currently facing humanity is heavy metal contamination. The purpose of this study is the removal of Strontium ions Sr(II) by using gamma radiation to create Starch/poly[2-(dimethylamino) ethyl methacrylate]/Bismuth (St/DMAEMA/Bi) nanocomposite. On the removal of Sr(II) ions, the effects of pH, contact time, adsorbent dose, and temperature were examined. The experimental data were fitted by Freundlich and Langmuir isotherm models. The results proved that the Langmuir isothermal model describes the absorption process well. To describe the adsorption kinetics of Sr(II) ions in compounds, the pseudo-second-order kinetic model is suitable. The thermodynamic results (ΔG° , ΔS° , and ΔH°) and isotherm investigations support the endothermic nature of the adsorption of Sr(II) ions on St/DMAEMA/Bi nanocomposite. Positive ΔH° values demonstrated the endothermic nature of the adsorption, while positive ΔS° values verified the increased randomness during the process, and the negative values of ΔG° show that the obtained experimental data best fits.

Keywords: Nanocomposite; Gamma radiation; Heavy metal ions; Adsorption; Pseudo-second order; Langmuir isotherm.

1. Introduction

The primary sources of heavy metal ions include nuclear fission plants, fertilizers, pesticides, fungicides, refineries, smoking, mining, the chemical industry, electroplating, paint, batteries, and other causes. Human organs that are harmed by heavy metal ion poisoning in aquatic systems include the lungs, brain, nose, tissue, kidneys, and central nervous system. [1]. Many wastewater treatment methods have been developed to remove heavy metal ions from wastewater, including solvent extraction, electrodialysis, filtration, photocatalysis, chemical precipitation, ion exchange, adsorption, membrane filtration, evaporation, electrolysis treatment technologies, chemical oxidation or reduction, electrodeposition, coagulation, sedimentation,

filtration, reverse osmosis, cementation, flocculation, and complexation. The amount of heavy metals present in solution and the cost of treatment are both taken into consideration when choosing a wastewater treatment method [2, 3]. Adsorption is seen as a superior technology for removing heavy metals from wastewater when compared to other conventional treatment methods because of its low cost, insensitivity to toxic pollutants, metal selectivity, ease of operation, stability, regenerative nature, flexibility and simplicity of design, and efficiency. Radiation-induced processes have several advantages over more traditional techniques [4]. In these processes, a backbone polymer that has absorbed radiation energy usually starts a free radical process. Catalysts, initiators, cross-linkers, and other

*Corresponding author e-mail: esraa.alshafei@yahoo.com E-mail: ghadancrrt@yahoo.com

Receive Date: 27 September 2023, Revise Date: 10 November 2023, Accept Date: 15 November 2023

DOI: 10.21608/EJCHEM.2023.239269.8677

©2023 National Information and Documentation Center (NIDOC)

potentially hazardous and difficult-to-remove materials are not required when producing hydrogel using radiation from a polymer solution.

Natural polymers have drawn attention because they are inexpensive, non-toxic, and potentially biodegradable materials that can also go through chemical changes. Wheat, tapioca, maize, and potatoes are just a few of the various resources that can be used to extract starch. Starch viscosity and association properties are occasionally altered chemically by incorporating a small number of ionic or hydrophobic groups into the starch molecules.

The ability of 2-(dimethylamino) ethyl methacrylate DMAEMA to form complexes with biological molecules and its sensitivity to pH and temperature made it an ideal choice for a polycationic component [5]. DMAEMA is a significant polymer that is used to create pH- and T-responsive hydrogels. Because DMAEMA molecules can take on different conformations depending on the pH of the environment, DMAEMA hydrogels are also pH-sensitive. The hydrophilicity of the chain is increased by the protonation of tertiary amines under acidic conditions, which causes a rapid expansion of the hydrogel. As a result, the hydrogel contracts when protonation is limited in an alkaline environment [6]. As a result, DMAEMA hydrogel has temperature- and pH-responsive properties, as well as a promising future for use in biosensors, contact lenses, pharmaceutical delivery systems, and other potential applications. The mechanical performance of DMAEMA hydrogel can be improved in a variety of ways, such as by creating novel molecular chain architectures, including nanoparticles, or by modifying microstructures [7–17].

To create various kinds of nanomaterials, the metal bismuth is frequently employed. These nanomaterials have qualities that make them appealing for a range of uses, including energy storage and conversion, electronics, sensors, and photothermal conversion. Because of their physiochemical properties and increased stability, researchers have been quite interested in nanomaterials based on bismuth [18, 19].

Various waste solutions contain strontium, depending on what the waste is used for and other environmental conditions. Spent nuclear fuel, high-level radioactive waste from spent nuclear fuel reprocessing, and other waste produced by nuclear accidents and nuclear weapon testing all contain significant amounts of strontium-90 (^{90}Sr). It is

simple to transfer strontium to both terrestrial and aquatic environments, and it remains for a long time because it is very soluble and has a long physical half-life. People can get strontium from eating, drinking, or inhaling it. Strontium behaves similarly to calcium in that it can have adverse effects on the bone marrow [20].

This study focuses on the removal of Sr(II) ions from wastewater by St/DMAEMA/Bi hydrogel nanocomposite, which is constructed by gamma radiation. According to contact time, pH, and initial metal ion concentration, the removal was investigated. So, we examined the mechanisms and adsorption kinetics of Sr(II) ion uptake by St/DMAEMA/Bi nanocomposite.

2. Experimental

El-Nasr Medical Supplies in Egypt supplied the starch delivery. We used DMAEMA (98%, Aldrich, 2-(dimethylamino) ethyl methacrylate). Bismuth (III) nitrate pentahydrate $\text{Bi}(\text{NO}_3)_3 \cdot 5\text{H}_2\text{O}$ from the Al-Gomhoria Company in Egypt, glycerol 99.5% was used without additional purification. NaOH was sourced from Merck. Distilled water was used to prepare the solutions. Strontium (II) Chloride hexahydrate ($\text{SrCl}_2 \cdot 6\text{H}_2\text{O}$) from Al-Nasr Co. Egypt.

Construction of St/DMAEMA/Bi hydrogel nanocomposite

A solution of 2% of St was prepared by adding 2 g St to 98 mL of H_2O , stirring at 80°C for one half hour, and then allowing it to cool to ambient. While stirring, different compositions of DMAEMA were added to the starch solution. 10 ml of glycerol was then added to 0.1g of $\text{Bi}(\text{NO}_3)_3 \cdot 5\text{H}_2\text{O}$. Glycerol was used, as a complexing agent, to increase the solubility of bismuth salt, as polyols that improve the solubility of metal ions by forming metal complexes. After mixing, the mixture was placed in glass tubes and subjected to gamma rays. The samples were exposed to 30 kGy of Cobalt-60 gamma rays at a radiation dosage rate of 1.2 Gy/sec. The Egyptian Atomic Energy Authority's (NCRRT) radiation facility performed the irradiation. The produced nanocomposite was sliced into small discs, put in water bath at 70°C to release the unreacted compound for 24 h and dried at 40°C .

Removal of Sr(II) ions

A known weight (m) of St/DMAEMA/Bi nanocomposite was deposited in a particular volume

(V) L of a known concentration (C_0) mg/L from Sr(II) ions rapidly shaken (250 rpm) for a certain time (t). Sr(II) ion concentration at time t (C_t) mg/L was evaluated by an atomic absorption spectrometer (BAC) (210VGP) in the presence of a strontium lamp with a hollow cathode of wavelength 460.7nm.

The removal percentage was calculated using Eq (1):-

$$\text{Removal}(\%) = \frac{(C_0 - C_t)}{C_0} \times 100 \quad (1)$$

Equation was used to calculate the quantity of adsorbed Sr(II) (mg/g) (q_e) (2):-

$$q_e = \frac{(C_0 - C_e)}{m} \times V \quad (2)$$

C_e represents the equilibrium concentration (mg/L).

3. Results and Discussion

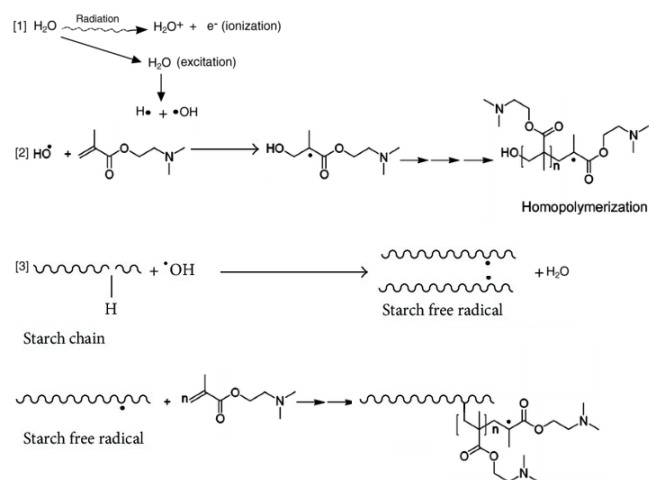
The synthesis of St/DMAEMA was prepared by the free radical copolymerization reaction, as seen in Scheme 1. When solutions containing DMAEMA and St are exposed to gamma radiation, free radicals are formed by the indirect effect of water. When gamma radiation is applied to water, it forms free radicals. One of these free radicals is hydrogen, and the other is the hydroxyl free radical. In contrast, the water's radiolysis by products might generate macro-radicals during the polymerization reaction's start stage, which is carried out by an indirect reaction. DMAEMA monomer's double bond can be combined with hydroxyl radicals produced during water radiolysis to create free radicals, which can subsequently interact with St. The St macro-radicals can combine with DMAEMA molecules (which are not radicals), causing branched chains to grow. In order to create polymer networks, the reaction's final step involves cross-linking the branched networks. This mechanism ignores some side reactions, such as the gamma-ray-induced polymerization of scissors.

3.1. Adsorption Study

3.1.1. Effect of pH Value

The pH value affects the material's surface properties and protonation level, which control how electrostatically interacting molecules interact. The variation in the percentage of Sr(II) ions removed by St/DMAEMA hydrogel and St/DMAEMA/Bi nanocomposite based on the medium's pH is depicted in Figure 1. By raising the pH of the solution from 1 to 6, Sr(II) ion uptake was increased. However, the removal percent dropped to pH 8. The maximum removal percent was achieved at pH 6.0, and the lowest value was obtained at pH 3 for both

St/DMAEMA and St/DMAEMA/Bi. This might be a result of amine protonation and hydroxyl groups taking place at low pH values and decreasing the binding sites for Sr(II) ions [21]. On the other hand, Sr(OH)₂ precipitation occurred at higher pH values (>6), preventing accurate adsorption calculations.



Scheme 1: The possible reaction mechanism.

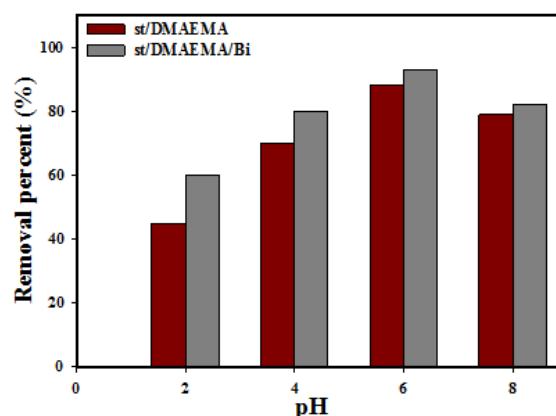


Fig.1: Effects of pH on the percentage of Sr (II) ions removed by St/DMAEMA hydrogel and St/DMAEMA/Bi nanocomposite.

3.1.2. Effect of the Concentration of Sr(II) ions

Figure 2 illustrates the percentage of Sr(II) ions removed by St/DMAEMA hydrogel and St/DMAEMA/Bi nanocomposite, depending on the concentration of Sr(II) ions. A high initial concentration of Sr(II) ions was found to increase the removal percent. Because there are more collisions between the metal ions and the adsorbent, it implies that more Sr(II) ions are removed from the solution [22]. When the concentration of ions on the adsorbent surface is too high, it becomes harder for them to react with adsorbent active groups [23]. It means that

the adsorbent is unable to remove much ion concentration at 150 mg/L. Bi nanoparticles enhance the adsorption characteristics of St/DMAEMA/Bi nanocomposite because nanoparticles have a large surface area responsible for improving the removal of Sr(II) ions.

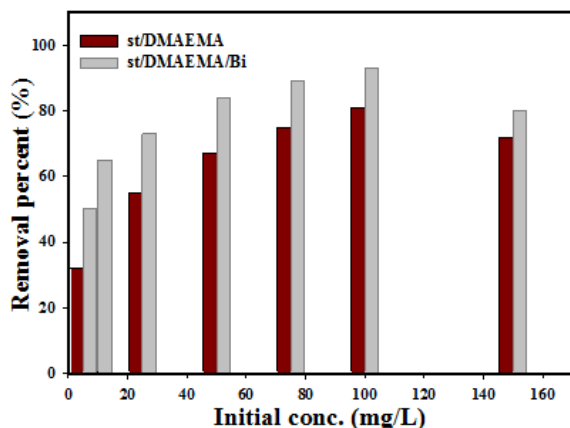


Fig. 2: Effect of initial Sr(II) ions concentration on the removal percentage by St/DMAEMA hydrogel and St/DMAEMA/Bi nanocomposite.

3.1.3. Impact of Adsorbent Dosage

Figure 3 illustrates the effect of removing percent of Sr(II) ions by St/DMAEMA hydrogel and St/DMAEMA/Bi nanocomposite. As the sorbent dosage was increased, the removal percentage increased, according to the results. Increasing the sorbent dose increases the surface area and the number of adsorption sites [24].

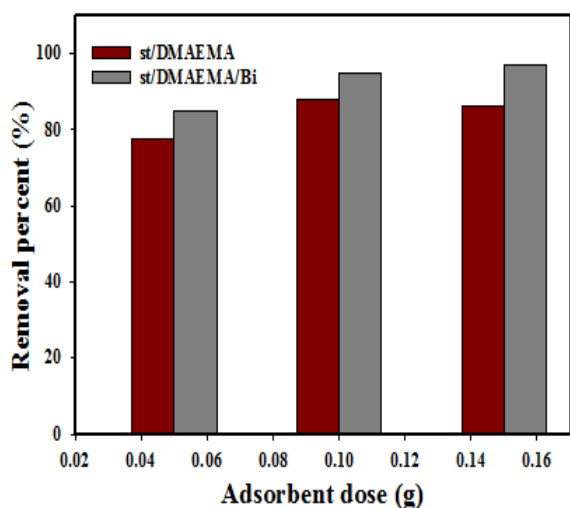


Fig. 3: Impact of adsorbent weight of St/DMAEMA hydrogel and St/DMAEMA/Bi nanocomposite for removal of Sr(II) ions.

3.1.4. Adsorption Isotherm

The interaction and equilibrium between the adsorbent and the adsorbed solution can be explained by the adsorption isotherm at a fixed temperature [25]. Finding the most effective model to explain the adsorption process is the main objective of studying isotherm data and fitting it to various isothermal models [26, 27]. To determine the type of adsorption, the Freundlich and Langmuir models were used. A monolayer adsorption taking place on the adsorbent's surface is assumed by the empirical Langmuir isotherm model. According to this model theory, on a solid surface, all of the active sites have the same amount of energy, which results in the relationship shown below:

$$\frac{ce}{qe} = \frac{1}{qmK_L} + \frac{ce}{qm} \quad (3)$$

C_e represents the equilibrium concentration of Sr(II) ions in the mixture (mg/L), q_e is the amount of Sr(II) ions adsorbed at equilibrium (mg/g), K_L is the equilibrium adsorption of the Langmuir constant (L/mg), and q_m is the equilibrium amount of Sr(II) ions in a monolayer (mg/g). The linear plot of C_e/q_e against C_e (Fig. 4a) and Table 2 display the parameters. The process of reversible and heterogeneous adsorption on a heterogeneous surface is described using the Freundlich isothermal model. It explains the multilayer adsorption. The equation below represents the Freundlich isotherm [28]:

$$\text{Log} q_e = \text{log} k_f + \frac{1}{n} \text{log} c_e \quad (4)$$

The constants K_f and n have been used, and the equilibrium adsorption capacity is represented by q_e (mg/g). Plotting the relationship between $\text{log} q_e$ and $\text{log} c_e$, as shown in Figure 4 and Table 1, lists the calculated parameters.

Compared to the Freundlich isotherm, the Langmuir isotherm more accurately represented the data when the correlation coefficients (R^2) for the two Sr(II) ion isotherms were compared with the results of fitting the adsorption data. The adsorbent becomes homogenized and forms a monolayer on its surface as a result of the adsorption process.

3.1.5. Effect of Temperature

At four different temperatures (25 °C, 30 °C, 40 °C, and 50°C), the St/DMAEMA hydrogel and St/DMAEMA/Bi nanocomposite's ability to remove Sr(II) ions was studied. Figure 5 shows that the amount of Sr(II) ions removed increased as the

temperature rose, showing that their adsorption onto adsorbents is endothermic [29,30].

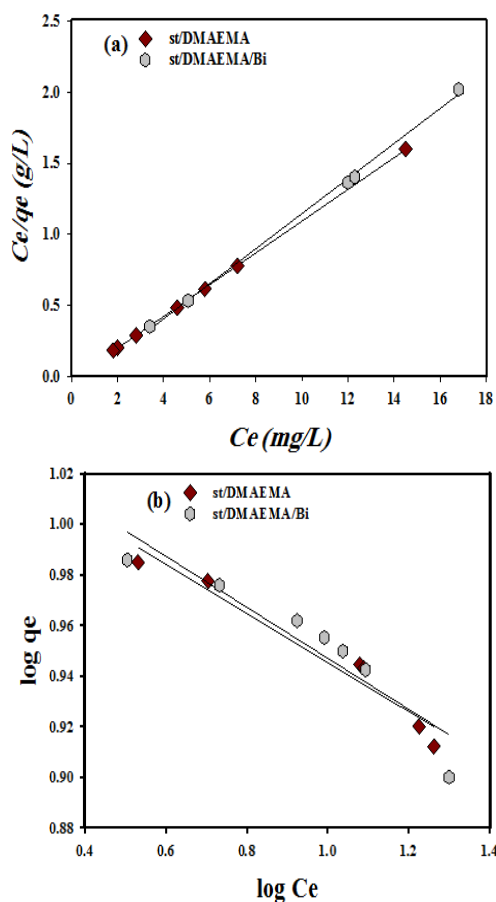


Fig. 4: The adsorption plots for Sr(II) ions by St/DMAEMA hydrogel and St/DMAEMA/Bi nanocomposite in Langmuir (a) and Freundlich (b).

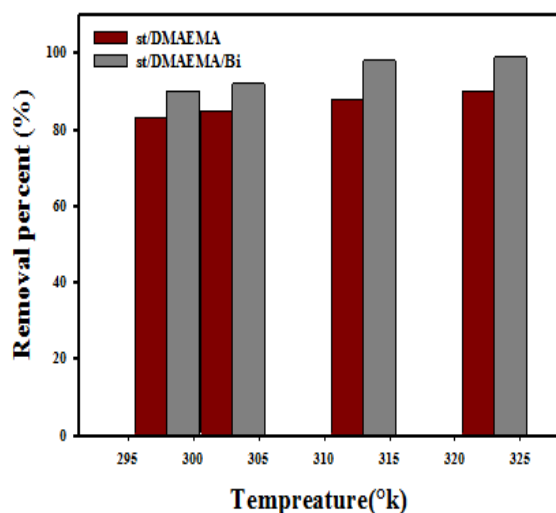


Fig. 5: The effect of temperature on the percentage of Sr(II) ions removed by St/DMAEMA hydrogel and St/DMAEMA/Bi nanocomposite.

3.1.6. Adsorption Kinetics

The most significant and frequently employed models for predicting adsorption kinetics are the pseudo-first-order and pseudo-second-order models [31]. According to the pseudo-first-order model,

$$\ln(q_e - q_t) = \ln q_e - k_1 t \quad (5)$$

Where k_1 (1/h) is the adsorption rate constant of pseudo-first order (g/mg min)

According to the concept of pseudo-second order,

$$t/q_t = 1/k_2 q_e^2 + t/q_e \quad (6)$$

k_2 (mg/gh) is the pseudo-second order constant of the adsorption rate (g/mg min).

Figure (6a) explains the plotted straight lines for $\ln(q_e - q_t)$ against t , and Figure (6b) illustrates the linear plots of t/q_t vs. t . Table 2 provides the calculated values for both equations. According to the results, compared to pseudo-1st order, the correlation portion R^2 was higher for pseudo-2nd order.

Compared to those achieved from the first order, the values of q from the pseudo-second order seem to be closer to the experimental data, which further ensures the pseudo-second-order model's desirable relationship. This proved that this model could be used to describe Sr(II) ions. As a result, the sorption rate of the available spots determines the adsorption medium. The rate-determining step of the adsorption process involves the concentration of both the adsorbent and the Sr(II) ions [32].

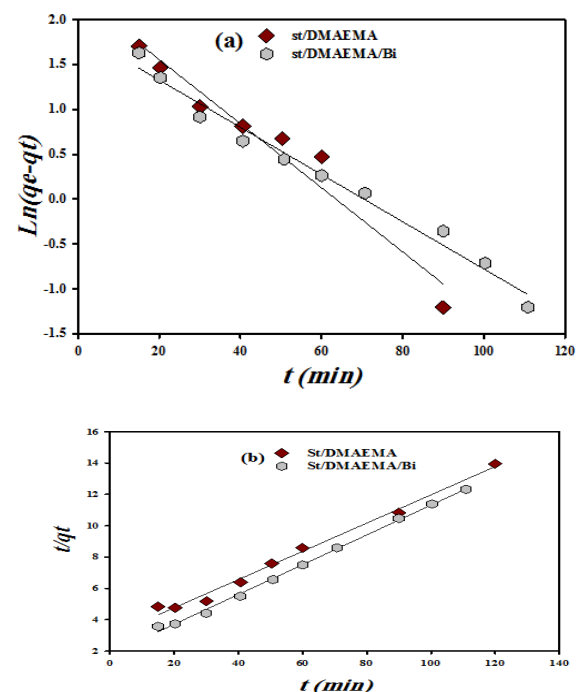


Fig. 6: Pseudo-1st order (a) and pseudo-2nd order (b) for the removal of Sr(II) ions by St/DMAEMA hydrogel and St/DMAEMA/Bi nanocomposite.

3.1.7. Influence of Time

Figure 7 looked into the effect of contact time on the removal of Sr(II) ions through a time range of 0 to 180 min. According to the research results, as the contact time increased from 0 to 180 min, the removal percentage for Sr(II) ions increased, and then it became slower as it approached equilibrium. This is because many active sites that were ready for absorption were discovered during the initial stages of removal [4]. Once every active site on the absorption surface is filled, the absorption rate falls until it eventually approaches equilibrium. After that, the absorption rate changes slightly, and its value is approximately constant at 180 min.

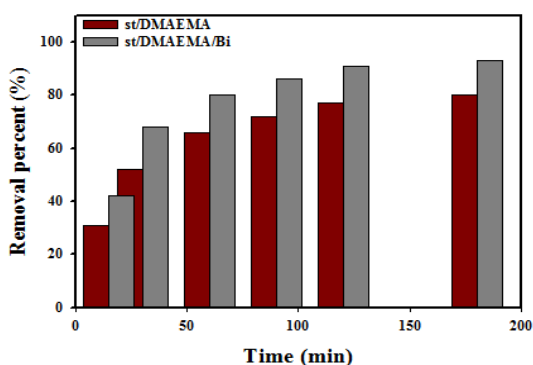


Fig. 7: Effect of time on the removal of Sr(II) ions by St/DMAEMA hydrogel and St/DMAEMA/Bi nanocomposite.

3.1.8. Adsorption Thermodynamics

By using Eq. 5, finding the thermodynamic parameter is possible by study Change in Gibbs free energy (ΔG°):

$$\Delta G^\circ = -RT \ln kd \quad (7)$$

$$kd = \frac{q_e}{c_e} \quad (8)$$

The distribution coefficient of thermodynamics is K_d , determined using Eq. 6, and the absolute temperature is T. R is known as the universal gas constant (8.314 J/mol K). By using the equilibrium values of q_e and C_e at various temperatures, kd was estimated. At various temperatures, the values of ΔG° were computed using Eq. 5. At these temperatures, the adsorption process is both possible and spontaneous, as shown by the negative values of ΔG° for Sr(II) ions at 303 °k, 313 °k, and 323 °k [33]. As temperature increased, the free energy of Sr(II) ions decreased (became more negative), resulting in more spontaneous adsorption. Values of ΔG° that are negative showed that the strontium removal process is stoichiometrically feasible and takes place spontaneously when using the adsorbents that are used. St/DMAEMA/Bi nanocomposite has a greater proclivity to adsorb at high temperatures, so that with rising temperatures, the change in Gibbs free energy shifts more negatively.

Table 1: The isotherm constants for the Langmuir and Freundlich models for Sr(II) ion adsorption by St/DMAEMA hydrogel and St/DMAEMA/Bi nanocomposite

	Langmuir parameters				Freundlich parameters		
	Q_m mg/g	K_L mg/L	R^2	R_L	n	k_f	R^2
St/DMAEMA	9.26	0.86	0.99	0.012	0.67	0.29	0.87
St/DMAEMA/Bi	58.9	0.16	0.998	0.059	0.77	0.45	0.85

Table 2: Pseudo-1st order and pseudo-2nd order constants on Sr(II) ions adsorption by St/DMAEMA hydrogel and St/DMAEMA/Bi .

Items	Pseudo-1 st order				Pseudo-2 nd order		
	q_e (exp.(mg/g))	q_e (cal.)(mg/g)	K_1 (min ⁻¹)	R^2	K_2 mg/g·h	q_{ecal} (mg/g)	R^2
St/DMAEMA	8.60	6.18	4.0×10^{-2}	0.91	0.0028	11.11	0.994
St/DMAEMA/Bi	10.0	5.05	3.0×10^{-2}	0.92	0.0051	10.42	0.998

Table 3: Thermodynamic parameters for Sr(II) ions removal

Items	Kd (mg/L)	ΔG° (KJ/mol)		
		303 (°K)	313 (°K)	323 (°K)
St/DMAEMA	0.833	- 2.099	- 2.168	- 2.237
	0.731	- 1.8423	- 1.903	- 1.964
	0.560	- 1.411	- 1.458	- 1.505
St/DMAEMA/Bi	0.717	- 1.807	- 1.866	- 1.926
	0.537	- 1.351	-1.396	- 1.440
	0.329	- 0.829	- 0.856	- 0.884

4. Conclusion

Experiments showed that the St/DMAEMA/Bi nanocomposite is highly effective in removing Sr(II) ions from contaminated water. The optimal pH for metal ion removal is 6, and absorption increases as Sr(II) ion concentration rises. According to the findings, the amount of adsorption increased with longer contact times until equilibrium was reached after 180 min. Pseudo-1st order and pseudo-2nd order models were used in kinetic studies under ideal conditions to estimate kinetic parameters. It was discovered that the pseudo-2nd order model fit the data more accurately than the Pseudo-1st order model. Freundlich and Langmuir models were able to be fitted with the experimental results. But it was discovered that the (R^2) for the Langmuir isotherm model was higher. The values of ΔG° that are negative show that the removal process is stoichiometrically feasible and takes place spontaneously.

5. Conflicts of Interest

“There are no conflicts to declare”.

6. References

- [1]. Perumal, S., Atchudan, R., Edison, T.N.J.I., Babu, R.S., Karpagavinayagam, P., Vedhi, C. A Short Review on Recent Advances of Hydrogel-Based Adsorbents for Heavy Metal Ions. *Metals J.* 2021, 11, 864.
- [2]. Abdel Halim, A., El-Ezaby, K.H., El-Gammal, M.I., Sabe, H.M. Removal of Fe²⁺ and Pb²⁺ ions from wastewater using rice husks-based adsorbents, *Egypt. Acad. Soc. Environ. Develop J.* 2019, 20 (1): 47-60.
- [3]. Khozemy, E.E., El-Nesr, E.M., Mahmoud, G.A. Radiation Synthesis of Novel Hydrogel Based on Wheat flour for Dyes Removal, *Arab J. Nucl. Sci. Appl.* 2020, 53, 2, 131-143.
- [4]. Nasef, Sh.M., El-Nesr, E.M., Kamal, F.H., Badawy, N.A., Sherbiny S.F. Gamma

Irradiation-Induced Preparation of Gum Arabic/ Poly (Vinyl Alcohol) Copolymer Hydrogels for Removal of Heavy Metal Ions from Wastewater, *Arab J. Nucl. Sci.& Applic.* 2020, 53, 1, 208-22.

- [5]. Bozbay, Orakdoge, N. Scaling Behavior and Structure-Property Relationships of Multifunctional Ternary-Hydrogels Based on N-Alkyl Methacrylate Esters: Property Tunability through Versatile Synthesis *Rabia, Macromol. Theory Simul.* 2022, 31,2100068.
- [6]. Tan, J., Chong, D., Zhou, Y., Wang, R., Wan, X., Zhang, J. Morphology evolution of stimuli-responsive tri-block copolymer modulated by polyoxometalates. *Langmuir.* 2018, 34, 8975–8982.
- [7]. Li, J., Xu, Z., Wu, W., Jing, Y., Dai, H., Fang, G. Nanocellulose/poly(2-(dimethylamino)ethyl methacrylate) interpenetrating polymer network hydrogels for removal of Pb(II) and Cu(II) ions. *Colloids Surf. A Physicochem. Eng. Asp.* 2018, 538, 474–480.
- [8]. Bhat, A., Smith, B., Dinu, C.Z., Guiseppi-Elie, A. Molecular engineering of poly(HEMA-co-PEGMA)-based hydrogels: Role of minor AEMA and DMAEMA inclusion. *Mater. Sci. Eng. C* .2019, 98, 89–100.
- [9]. Fu, F.F., Chen, Z.Y., Zhao, Z., Wang, H., Shang, L.R., Gu, Z.Z. and Zhao Y.J., Bio-inspired self-healing structural color hydrogel. *PNAS.* 2017, 114(23), 5900–5905.
- [10]. Sun, A.K., Shen, Y.L., Wu, Z.Z., Wang, D.Z. N-doped MoP nanoparticles for improved hydrogen evolution. *Int. J. Hydrog. Energy.* 2017, 42(21), 14566–14571.
- [11]. Deng, X.T., Yin, S.F., Wu, X.B., Sun, M., Li, Z.Q. Scal-able preparation of PtPd/carbon nanowires in the form of membrane as highly stable electrocatalysts for oxygen reduction reaction. *Int. J. Hydrog. Energy.* 2019, 44(5), 2752–2759.
- [12]. Jian, H.G., Luo, J., Tang, X.M., Li, X., Yan, C. Influence of microstructure on fatigue crack

- propagation behaviors of an aluminum alloy: Role of sheet thickness. *Eng. Fract. Mech.* 2017, 180, 105–114.
- [13]. Chen, L.J., Chen, H., Wang, Z., Gong, X.Z., Chen, X.H. Self-supporting lithiophilic N-doped carbon rod array for dendrite-free lithium metal anode. *J. Chem. Eng.* 2019, 363, 270–277.
- [14]. Hu, Z.L., Qin, S.L., Huang, Z., Zhu, Y.R., Xi, L.J. Step-wise synthesis of graphene oxide-wrapped magnetic composite and its application for the removal of Pb(II). *Arab J Sci Eng.* 2017, 42(10), 4239–4247.
- [15]. He, Y., Xiang, K.X., Zhou, W., Zhu, Y.R. and Chen, X.H., Folded-hand silicon/carbon three-dimensional networks as a binder free advanced anode for high-performance lithium-ion batteries. *J. Chem. Eng.* 2018, 353, 666–678.
- [16]. Xie, S.W., Gong, G., Song, Y., Tan, H.H., Zhang, C.F., Li, N., Zhang, Y.X., Xu, L.J., Xu, J.X. and Zheng, J., Design of novel lanthanide-doped core-shell nanocrystals with dual up-conversion and down-conversion luminescence for anti-counterfeiting printing. *J. Chem. Soc., Dalton Trans.* 2019, 48, 6971–6983.
- [17]. Li, J.M., Hu, C.S., Shao, J.M., Li, H.J., Li, P.Y., Li, X.C., He, W.D. Fabricating ternary hydrogels of P(AM-co-DMAEMA)/PVA/-CD based on multiple physical crosslinkage. *Polym.* 2017, 119, 152–159.
- [18]. Kazemi, N.M., Yaqoubi, M. Green Synthesis and Characterization of Bismuth Oxide Nanoparticle Using Mentha Pulegium Extract, *IJPR* 2020, 19 (2): 70-79.
- [19]. Sivasubramanian, P.D. Chang, J.H., Nagendran, S., Dong, Ch.D., Shkir, M., Kumar, M. A review on bismuth-based nanocomposites for energy and environmental applications, *Chemosphere.* 2022, 307(Pt 1):135652.
- [20]. İnan, S. Inorganic ion exchangers for strontium removal from radioactive waste: a review, *JRNC.* 2022, 331:1137–1154.
- [21]. Moreno-Sader, K., García-Padilla, A., Realpe, A., Acevedo-Morantes, M., Soare J.B. P. Removal of Heavy Metal Water Pollutants (Co²⁺ and Ni²⁺) Using Polyacrylamide/Sodium Montmorillonite (PAM/Na-MMT) Nanocomposites, *ACS Omega* 2019, 4, 10834–10844.
- [22]. Ghada A. Mahmoud, Mohamed Abdel-Geleel, Nagwa A. Badway, Samia A. Abo Farha, Esraa A. Alshafei. Characterization and Adsorption Properties of Starch-Based Nanocomposite for Removal of Simulated Low-Level Radioactive Waste, *Starch/Stärke* 2023, Vol. 75.
- [23]. Ghada A. Mahmoud , Samia E. Abdel-Aal, Nagwa A. Badway , Samia A. Abo Farha, Esraa A. Alshafei. Radiation synthesis and characterization of starch-based hydrogels for removal of acid dye. *Starch/Stärke* 2013, Vol. 65, 1–10.
- [24]. Gran, S., Aziz, R., Rafiq, M.T., Abbasi, M., Qayyum, A., Elnaggar, A.Y., Elganzory, H.H., El-Bahy, Z.M., Hussein, E.E. Development of Cerium Oxide/Corn cob Nanocomposite: A Cost-Effective and Eco-Friendly Adsorbent for the Removal of Heavy Metals. *Polym.* 2021, 13, 4464.
- [25]. Al-Ghouti, M.A., Al-Absi, R.S. Mechanistic understanding of the adsorption and thermodynamic aspects of cationic methylene blue dye onto cellulosic olive stones biomass from wastewater. *Sci. Rep.* 2020, 10(1), 1-18.
- [26]. Ayawei, N., Ebelegi, A.N., Wankasi, D. Modelling and interpretation of adsorption isotherms. *J. Chem.*, 2017.
- [27] Shih, C., Park, J., Sholl, D.S., Realff, M.J., Yajima, T., Kawajiri, Y. Hierarchical Bayesian estimation for adsorption isotherm parameter determination. *Chem. Eng.Sci.* 2020, 214, 115435.
- [28]. Al-Ghouti, M.A., Da'ana, D.A. Guidelines for the use and interpretation of adsorption isotherm models: *J. Hazard. Mater.* 2020, 393, 122383.
- [29]. Manechakr, P., Karnjanakom, S. Adsorption behaviour of Fe(II) and Cr(VI) on activated carbon: surface chemistry, isotherm, kinetic and thermodynamic studies. *J Chem. Thermodyn.* 2017, 106, 104–112.
- [30]. Sharma, G., Kumar, A., Naushad, M., García-Peñas, A., Al-Muhtaseb, A.H., Ghfar, A.A., Sharma, V., Ahamad, T., Stadler, F.J. Fabrication and characterization of gum arabic-cl-poly(acrylamide) nanohydrogel for effective adsorption of crystal violet dye. *Carbohydr. Polym.* 2018, 202, 444–453.
- [31] Kukwa, R.E., Kukwa, D.T., Oklo, A.D., Ligon, T.Th., Ishwah, B., Omenka J.A. Adsorption Studies of Silica Adsorbent Using Rice Husk as a Base Material for Metal Ions Removal from

-
- Aqueous Solution. *Am. J. Chem. Eng.* 2020, 8, 2, 48-53.
- [32]. Gran, S., Aziz, R., Rafiq, M.T., Abbasi, M., Qayyum, A., Elnaggar, A.Y., Elganzory, H.H., El-Bahy, Z.M., Hussein, E.E. Development of Cerium Oxide/Corncob Nanocomposite: A Cost-Effective and Eco-Friendly Adsorbent for the Removal of Heavy Metals. *Polym.* 2021, 13, 4464.
- [33]. Naushad, M., Ahamad, T., Al-Maswari, B.M., Alqadami, A.A., Alshehri, S.M. Nickel ferrite bearing nitrogen-doped mesoporous carbon as efficient adsorbent for the removal of highly toxic metal ion from aqueous medium. *Chem Eng J.* 2017, 330, 1351–1360.